Research Article

Journal of the Optical Society of America A

OPTICS, IMAGE SCIENCE, AND VISION

Combinations of generalized lenses that satisfy the edge-imaging condition of transformation optics

Tomáš Tyc,[1] Jakub Bělín,[2] Stephen Oxburgh,[2] Chris D. White,[3] Euan N. Cowie,[2] and Johannes Courtial[2,*]

[1]Institute of Theoretical Physics and Astrophysics, Masaryk University, Kotlarska 2, 61137 Brno, Czech Republic
[2]School of Physics & Astronomy, College of Science & Engineering, University of Glasgow, Glasgow G12 8QQ, UK
[3]Centre for Research in String Theory, Queen Mary University of London, 327 Mile End Road, London E1 4NS, UK
*Corresponding author: Johannes.Courtial@glasgow.ac.uk

Received 16 September 2019; accepted 6 November 2019; posted 14 November 2019 (Doc. ID 378040); published 24 January 2020

We recently introduced the edge-imaging condition, a necessary condition for all generalized lenses (glenses) [J. Opt. Soc. Am. A 33, 962 (2016)] in a ray-optical transformation-optics (RTO) device that share a common edge [Opt. Express 26, 17872 (2018)]. The edge-imaging condition states that, in combination, such glenses must image every point to itself. Here we begin the process of building up a library of combinations of glenses that satisfy the edge-imaging condition, starting with all relevant combinations of up to three glenses. As it grows, this library should become increasingly useful when constructing lens-based RTO devices.

https://doi.org/10.1364/JOSAA.37.000305

1. INTRODUCTION

Transformation optics (TO) [1,2] is a way to design optical devices whose inside appears to be distorted. In the case of the famous invisibility cloak [2], a volume inside the device—and any object it contains—appears to approach zero size to any observer located anywhere outside the device, while the device itself is invisible. This can be achieved by taking a volume of empty space, in which light rays travel along straight lines, and distorting the space along with the light-ray trajectories using a coordinate transformation (or mapping). Such distortions of light-ray trajectories can, at least in principle, be achieved with solid volumes of material with spatially varying optical properties. The empty space is called *virtual space*, and the distorted space is called *physical space*.

The mapping between the physical space and virtual space maps not only positions on the trajectories of individual light rays, but also the positions where multiple rays intersect. In other words, positions are being imaged from physical space to a corresponding position in virtual space. The (real or virtual) actual position where light rays travelling inside the device intersect is in physical space; the corresponding virtual-space position is then the (again real or virtual) intersection point of those parts of the same light rays that lie outside the device, and thus the position where the corresponding physical-space position appears for an observer located outside of the device. As our definition of a TO device we use the existence of a unique mapping from any position in physical space to a corresponding virtual-space position. Note that we do not dwell here on the distinction between devices that map waves and those that only map rays, so-called ray-optical TO (RTO) devices.

Our own approach to TO stems from our ability to construct thin sheets that perform very general *integral imaging*. In stigmatic imaging, all rays that pass through the object position before passing through an imaging device intersect again after passing through the device at the image position. In integral imaging, it is not all individual light rays that intersect at the object and image positions, but the centers of ray *bundles* [3], resulting in a lower image quality than in stigmatic imaging. Many stigmatic-imaging sheets cannot be realized physically as they would result in non-physical light-ray fields [4], but the corresponding integral-imaging sheets *can* be realized.

The most general planar, light-ray direction-changing, sheet that stigmatically images all space is called a *glens*, a generalization of an idealized thin lens [5]. (Curved interfaces that image all space, or even just a suitably defined volume of space, can only perform the trivial identity mapping [6].) The mapping between the object and image space performed by glenses is so general that structures of glenses can form omni-directional transformation-optics devices [7–9]. One particular type of our sheets, generalized confocal lenslet arrays (GCLAs) [10],

can function as "integral glenses": imaging sheets with the same mapping between the object and image space as glenses, but which perform integral imaging instead of stigmatic imaging [11]. GCLAs are pairs of microlens arrays that share a common focal plane so that the structure is an array of micro-telescopes, which is why we also call them *telescope windows*. In a sense, each telescope forms one *pixel* of the sheet, and for this reason, we refer to the light-ray direction change effected by such sheets as *pixellated generalized refraction*. In addition to the lower image quality associated with integral imaging, there are additional shortcomings associated with the design of telescope windows, such as diffraction and absorption [12].

After constructing glens-based TO devices, we decided to avoid the shortcomings discussed above by searching for special cases in which all glenses are actually ideal thin lenses. This was done in two steps: first, we designed a device in which only a few of the glenses were lenses [9], and then one in which *all* glenses were lenses [13]. The resulting lens-only TO device can be considered an omnidirectional lens [13], that is, a lens with a field of view of 4π, or an invisibility cloak [14]. Ideally, the imaging is stigmatic, but our arguments also apply when this is not the case, for example when it is integral, like in our devices based on telescope windows, or suffers from other aberrations, such as in devices based on actual (i.e., non-ideal) lenses.

We designed all our TO devices based on glenses [9] or lenses [13,14] by using *identity-mapping conditions* on certain combinations of optical components, that is, the requirement that any object position is imaged to the same position again—the mapping between any object position and its image position is the identity map. Specifically, all optical components encountered along any closed loop in a TO device must image every point to itself, a condition we call the *loop-imaging condition* for the loop. According to the *loop-imaging theorem*, the loop-imaging condition needs to be satisfied for every closed loop in a glens structure for that glens structure to be a TO device. Thankfully, in the case of glens structures, it is not necessary to test the loop-imaging condition for *every* closed loop; instead, it is merely necessary to test a set of *edge-imaging conditions*, one for every edge in the structure where glenses meet. The edge-imaging condition is the identity-mapping condition applied to the combination of all glenses that share a common edge.

With the aim of facilitating the construction of lens-based and glens-based TO devices, we derive here from the edge-imaging condition rules for the placement of the nodal points, and we start building up a "library" of glens-based building blocks for TO devices by applying the edge-imaging condition to different combinations of glenses. The results allow quick and easy rejection of unsuitable designs and calculation of all glens parameters.

This paper is structured as follows. We start with reviews of glenses (Section 2) and of the loop-imaging and edge-imaging conditions (Section 3). In Section 4, we derive conditions on the positions of the nodal points in glens combinations that satisfy the identity-mapping condition. In Section 5, we investigate specific combinations of glenses that intersect along a common edge, starting with few glenses and working toward more glenses. As a guide to applying our results, we outline, in Section 6, our use of the results in designing ideal-lens TO devices. Section 7 concludes the main part of the paper. The appendixes state and prove several useful theorems about glenses and lenses.

2. REVIEW OF GLENSES

A glens is a generalization of an ideal lens so that the focal lengths on the two sides can be different from each other [5]. As a glens is therefore no longer mirror symmetric with respect to the glens plane, it is important to be able to identify the two different sides of the glens, specifically which side each focal length refers to. This is done by placing the axis of a new coordinate called a on the optical axis so that the glens lies in the $a = 0$ plane. The focal lengths are then identified by the a coordinate of the corresponding focal point, whereby the focal length that refers to −ve space (the space of light rays travelling on the glens' side where $a < 0$) is called f^-, and that referring to +ve space is called f^+. Note that, by this convention, an ideal lens of focal length f is a glens with focal lengths $f^+ = f$ and $f^- = -f$.

An important difference between an ideal lens and a glens is the position of the nodal point N, the cardinal point lying on the optical axis with the property that the direction of light rays passing through this point do not change direction at the (g)lens: in the case of an ideal lens, N coincides with the principal point; in the case of a glens, N can lie anywhere on the optical axis. The a coordinate of N, the *nodal distance* n, can be found by the equation

$$n = f^+ + f^-. \tag{1}$$

It is clear that the nodal distance of an ideal lens is zero, so the nodal point lies in the plane of the ideal lens, specifically the position where this is intersected by the optical axis, i.e., it coincides with the ideal lens' principal point.

3. MAPPING CONDITIONS IN TO DEVICES

Consider a TO device constructed from glenses. The inner region of the device is divided into cells by the glenses. Figure 1 shows the generic structure of such a device; it is drawn in 2D, but our considerations equally apply in 3D. In 2D, intersecting glenses meet at points, namely the vertices of the polygonal cells. In 3D, glenses intersect in lines, namely the edges of the polyhedral cells.

A glens maps straight lines to straight lines; such a mapping is called a collineation. The glens separating cells i and j images from the space of cell i to the space of cell j according to the collineation c_{ji}. (Note that the indices are in the order of image cell first and object cell second. This is to make expressions that describe multiple mappings more readable.) Clearly, the mapping that describes imaging from the space of cell j to the space of cell i is the inverse of c_{ji}: $c_{ij} = c_{ji}^{-1}$.

Now consider light rays passing through a position P_i in the space of cell i. We allow this position to be real, if the actual light-ray-trajectory segments in cell i intersect, or virtual, if the straight-line continuations through those segments intersect, so "a position in the space of cell i" can actually lie outside of cell i.

The light rays travel from cell i to the outside, which we call cell 0, via two intermediate cells j and k (the generalization to different numbers of intermediate cells is obvious). Imaging of any position in the space of cell i to the outside space is then

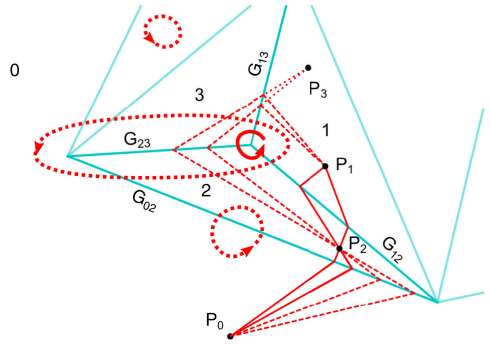

Fig. 1. Schematic of part of a transformation-optics device formed by glenses (cyan lines). The glenses divide the inside of the device into cells, three of them numbered 1 to 3; cell 0 is the outside of the device. The glens separating cells i and j ($i < j$) is labelled G_{ij}. A few light rays that start from a point light source at position P_1 inside the space of cell 1 and travel to its image position in outside space, P_0, are shown; rays that travel through glenses G_{12} and G_{02} are shown as solid red lines, and those that travel through glenses G_{13}, G_{23}, and G_{02} are shown as dashed red lines. P_2 and P_3 are intermediate images in the space of cells 2 and 3, respectively. A number of closed loops are shown as thick red arrows, the one around the common vertex between cells 1, 2, and 3 as a solid arrow, others as dotted arrows. The loops can contain any number of vertices, including none. For simplicity, the figure is drawn in 2D; in 3D, the polygonal cells from the 2D case become polyhedral cells, and the vertices become edges.

described by a successive application of the mappings from the space of cell i to the space of cell j, from there to the space of cell k, and from there to the space of cell 0. If we describe the position P_i in the space of cell i by the vector $\mathbf{P}_i$, then the position vector of its image in the outside space, i.e., the space of cell 0, is

$$\mathbf{P}_0 = c_{0k}c_{kj}c_{ji}\mathbf{P}_i. \tag{2}$$

The expression $c_{0k}c_{kj}c_{ji}$, therefore, describes the mapping of any physical-space position in the space of cell i through the spaces of cells j and k to the corresponding position in the outside space.

We are interested in the situation when the mapping from the space of cell i to the outside space does not depend on precisely which cells the light rays pass through on their way from cell i to the outside. If, in this case, we place a point light source at the position P_i inside cell i, then P_0 is the position where they appear to intersect to an outside observer, and this position is independent of the path the light rays have taken, and therefore unique. P_0 is therefore the virtual-space position corresponding to the physical-space position P_i. The mapping from the space of cell i to the outside space then no longer depends on the path taken by the light rays; we call this unique mapping (which is again a collineation) C_i.

Consider now two routes light-ray trajectories can take between the position P_1 in the space of cell 1 in Fig. 1 to the outside. The first route passes through cell 2 (through glenses G_{12} and G_{02}), the second through cells 3 and 2 (through glenses G_{13}, G_{23}, and G_{02}). As we require the mapping from the space of cell 1 to the outside to be unique, and therefore independent of the cells through which light rays pass,

$$c_{02}c_{21} = C_1 = c_{02}c_{23}c_{31}. \tag{3}$$

Multiplying both sides of this equation by $(c_{02}c_{21})^{-1} = c_{12}c_{20}$ from the left, we find that

$$I = c_{12}c_{23}c_{31}, \tag{4}$$

where I is the identity mapping. The right-hand side describes the mapping encountered along a closed loop, starting and finishing in cell 1, circumnavigating the common vertex between cells 1, 2, and 3, and shown in Fig. 1 as a thick solid arrow. The requirement that the combination of the glenses encountered along the closed loop images every point to itself is called the *loop-imaging condition* for that particular loop. Similarly, we can pick loops that start in any cell and perform a circumnavigation of any number of vertices, thereby arriving at the *loop-imaging theorem*: *the loop-imaging condition is satisfied for any closed loop in a TO device.*

Note that the closed loops can contain any number of vertices (in 2D) or edges (in 3D; in the following, we use the terms appropriate for the 3D case), including none; a few examples are shown in Fig. 1, drawn as dashed thick arrows. However, we normally concentrate on loops that contain one edge. The loop-imaging condition for any such loop—the *edge-imaging condition* for the particular edge encircled by the loop—requires that the combination of all glenses that meet at that particular edge images every point to itself. Compared to larger loops, such minimalist loops lead to simpler equations derived from the loop-imaging condition while still expressing the essence of the TO device they describe: in Ref. [13], the *edge-imaging theorem* was shown, which states that the requirement that the edge-imaging conditions for all edges in a structure are satisfied is a sufficient condition for the structure to be a TO device.

We note that the requirement for a combination of glenses to image every position back to itself is equivalent to the requirement that the combination of glenses restores every light ray to its original straight-line trajectory. This can easily be seen by considering two different positions that lie on the trajectory of a light ray before it intersects the first glens. For the glens combination to image an object position to its corresponding image position, it must redirect any incident light ray that passes through the object position so that the outgoing light ray passes through the image position. As the loop-imaging condition states that every point is imaged to itself, the outgoing light ray therefore has to pass through both positions through which the incident ray passed, which means that the trajectory of the outgoing light ray has to be identical (but possibly in the opposite direction) to that of the incoming light ray.

We note that we can apply this formulation of the loop-imaging condition to standard TO devices. The loop-imaging then concerns the light-ray-direction change due to the optical material properties encountered along a given closed loop in a TO device: after passing through any closed loop in a TO device, a light ray has to have the same direction that it had initially. Note that this is not satisfied in the invisible lens [15,16], for example, in which trajectories can intersect themselves at an angle, and which is therefore not a TO device.

In the following, we apply the edge-imaging condition to combinations of different numbers of glenses that, unless otherwise stated, share a common edge. Clearly, the edge-imaging

condition is trivially satisfied for zero glenses. The case of a single glens is also trivial: the effect of the combination of all glenses intersecting at the edge can be the identity map only if the single glens itself maps according to the identity map, i.e., if its parameters represent a lens with infinite focal length—a transparent window. If more glenses are involved, the situation becomes more complicated, and this is discussed in the following sections.

4. CONDITIONS ON THE NODAL POINTS

In previous sections, we reviewed identity-mapping conditions for the optical elements encountered along an arbitrary closed loop in a TO device (the loop-imaging condition) and along a closed loop around an edge where several glenses meet in a TO device (the edge-imaging condition). Here we consider the consequences of the identity-mapping condition on the nodal-point positions in combinations of glenses. We do not make the assumption that all the glenses in the combinations we consider here intersect in a common edge.

We start by deriving conditions on the nodal points of different combinations of glenses. We consider only combinations in which no two neighboring glenses lie in the same plane, as such co-planar glenses can be described as a single glens in the same plane (see Appendix B). (Note that non-neighboring glenses can lie in the same plane, namely on opposite sides of the common edge.) We will see that more glenses mean more relaxed conditions on the nodal points. These conditions can be used to test, quickly, whether or not a given combination of glenses can be a TO device.

For the case of two glenses, consider Fig. 2(a). Light ray 1 is chosen so that it is incident on G_1 at a point other than any point where G_1 and G_2 intersect. We use the fact that, in order to image every point to itself, the glens combination must restore every light ray back to its original trajectory. As glenses do not offset light rays on transmission, this is possible only if G_1 and G_2 do not alter the ray's direction at all. This implies that the nodal points of G_1 and G_2, N_1 and N_2, lie somewhere on the ray trajectory. Repeating the argument with ray 2, similarly chosen to ray 1 with the additional requirement that it intersects ray 1, implies that both N_1 and N_2 lie on the intersection between rays 1 and 2. Repeating the argument with ray 3, again similarly chosen to ray 1 but with the additional requirement that it does not pass through any intersection point between rays 1 and 2, implies that N_1 and N_2 also lie on ray 3. This contradicts our earlier deduction that N_1 and N_2 lie on the intersection of rays 1 and 2, and we have thus shown that our assumptions are wrong. Specifically, as we show in Section 5.A, there are no combinations of two glenses that do not lie in the same plane and that satisfy the identity-mapping condition.

Figure 2(b) shows a combination of three glenses that performs the identity mapping. N_1 is the nodal point of the first glens. We use again the fact that the identity-mapping requirement is equivalent to restoring every light ray back to its original trajectory. We consider ray 1 in Fig. 5(b), chosen so that it passes through N_1 and that it intersects G_2 and G_3 at different points. Because N_1 is the nodal point of G_1, the ray passes straight through G_1 and continues to G_2. Transmission through G_2 and G_3 must therefore restore the ray to its original straight-line

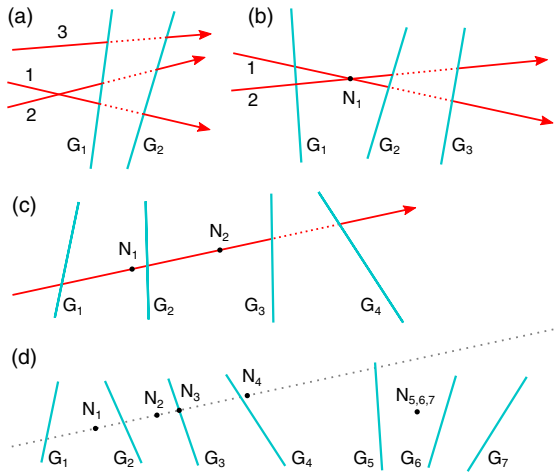

Fig. 2. Diagrams used in the derivation of conditions on the nodal points in combinations of (a) two, (b) three, (c) four, and (d) six glenses that satisfy the identity-mapping condition. The cyan lines marked as G_i indicate the plane of the i-th glens, and N_i is the position of the nodal point of the i-th glens. The red arrows show the trajectories of light rays that pass through the nodal point of the first glens and, in (c), also that of the second glens. In (d), the combination of glenses G_1 to G_4 satisfies the identity-mapping condition, and so does the combination of glenses G_5 and G_6. The nodal points of G_1 to G_4 and N_1 to N_4 lie on the dotted line. Glenses G_5, G_6, and G_7 share a common nodal point, $N_{5,6,7}$.

trajectory, which is possible only if G_2 and G_3 do not alter the ray's direction either. This, in turn, implies that the nodal points of glenses 2 and 3, N_2 and N_3, lie on the straight-line trajectory of ray 1. Like in the two-glens case above, repeating the above argument with ray 2, similarly chosen to ray 1 but with the additional requirement that rays 1 and 2 intersect, leads to the conclusion that N_2 and N_3 also lie on ray 2. N_2 and N_3 therefore lie at the point where rays 1 and 2 intersect. But rays 1 and 2 were both chosen to pass through N_1, so their intersection point coincides with N_1. This implies that all three glenses share a nodal-point position.

With the help of Fig. 2(c), we can derive a condition on the nodal points of four glenses that, in combination, image every point back to itself. As in the preceding cases, we use the fact that they have to restore every light ray back to its original trajectory. Consider a light ray that is incident along the straight line that contains the nodal points of glenses 1 and 2, N_1 and N_2, and that therefore passes undeviated through glenses 1 and 2. By the same argument as before, the ray also has to pass through glenses 3 and 4 undeviated to continue along its original trajectory. This, in turn, is only possible if the nodal points of glenses 3 and 4 lie on the light-ray trajectory. But as that trajectory also contains the nodal points of glenses 1 and 2, and as it is a straight line, the nodal points of all four glenses must lie on that same straight line. Unless N_1 and N_2 coincide, we cannot then pick a different light ray that passes through N_1 and N_2, as there is only one such ray, and so the above statement of all four nodal points lying on a straight line is all we can say. For the special case in which N_1 and N_2 coincide, the same argument applied to a different ray through N_1 and N_2 results again in the conclusion that all four glenses share a nodal-point position.

From the cases discussed so far, we observe a general pattern: the larger the number of glenses, the less restrictive the conditions on the nodal points. Indeed, if the number of glenses is greater than some minimum number, then the nodal points no longer have to lie on a straight line. This minimum number is ≤ 6, as we can easily construct an example of a combination of six glenses that satisfies the identity-mapping condition and in which the nodal points do not all lie on a straight line, as follows. Figure 2(d) shows a group of four glenses, G_1 to G_4, that, on its own, satisfies the identity-mapping condition, and a group of three glenses, G_5 to G_7, that, again on its own, also satisfies the identity-mapping condition. The four-glens combination is chosen so that its nodal points do not coincide. In combination, these seven glenses therefore map every point to itself. We now move the groups relative to each other so that glens G_4 of the first group is co-planar with glens G_5 of the second, and so that the (common) nodal point of the three-lens group does not lie on the straight line on which the nodal points of the four-lens group lie. The two co-planar glenses can be combined into an equivalent single glens (see Appendix B). The resulting combination of six glenses therefore satisfies the identity-mapping condition, and the nodal points do *not* lie on a straight line. (One might be tempted to repeat this construction with two groups of three lenses, arrange these so that two glenses—one from each group—become co-planar, and combine these co-planar glenses into a single glens. Note that the nodal point of the equivalent glens lies on the straight line through the nodal points of the individual glenses (see Appendix B), which implies that the nodal points of the resulting combination of five glenses lies on a straight line.)

5. GLENS COMBINATIONS THAT SATISFY THE EDGE-IMAGING CONDITION

We now specifically consider combinations of glenses that satisfy the edge-imaging condition. This implies that they share a common edge. Figure 3 shows the geometry of such glens combinations.

A. Two Glenses

It is instructive first to consider briefly two arrangements of two lenses that obviously satisfy the identity-mapping condition.

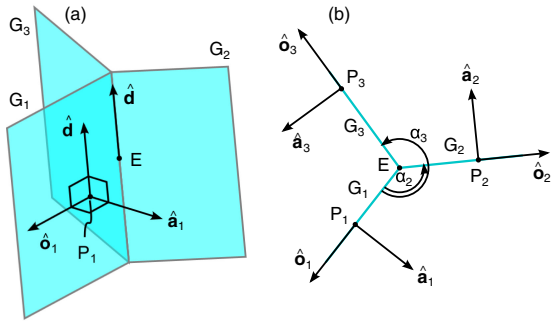

Fig. 3. Geometry of n glenses sharing a common edge, drawn here for $n = 3$. (a) 3D view; (b) orthographic projection in a plane perpendicular to the edge. E is a point on the edge; $\hat{\mathbf{d}}$ is a unit vector in the direction of the edge; α_{ij} is the angle from glens i to glens j.

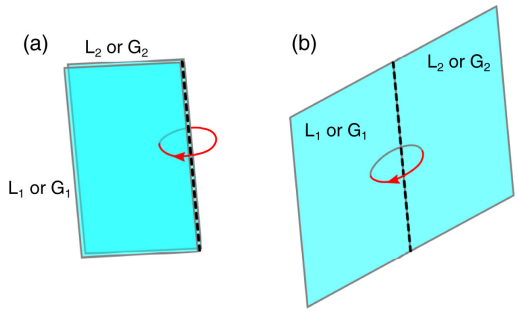

Fig. 4. Combinations of two lenses, L_1 and L_2, or two glenses, G_1 and G_2, that satisfy the edge-imaging condition. The two possible cases are (a) $\alpha_{12} = 0$ and (b) $\alpha_{12} = \pi$. The common edge for which the edge-imaging condition is satisfied is highlighted by a thick dashed line. A closed loop around each of these edges is shown as a red arrow.

The first arrangement [Fig. 4(a)] comprises two lenses in the same plane that cancel each other's effects, which means the second lens is identical to the first lens in all aspects (including position) other than the sign of the focal length. The second arrangement [Fig. 4(a)] is the case of a loop that intersects a single lens twice, which can be considered as a special case of two lenses intersecting along a line threading the loop, whereby the two lenses are two parts of the lens that are formed if the lens is divided along the line. The total effect of circumnavigating the loop is then the identity mapping, as the mapping performed on crossing the lens the first time is reversed on passing through the lens again in the other direction. The following calculation finds the analogous arrangements of two glenses and shows that there are no other arrangements that satisfy the identity-mapping condition.

Figure 3 shows the geometry of glenses sharing a common edge; we consider here such an arrangement with two glenses. Without loss of generality, we can translate our coordinate system so that the origin coincides with the position E on the intersection line between the glenses, and rotate it so that the vector $\hat{\mathbf{d}}$ in the direction of the intersection line points in the positive z direction and $\hat{\mathbf{a}}_1$, the first glens's optical axis, points in the positive x direction. The optical axis of the second glens is rotated by an angle α_{12} about the z-axis with respect to that of the first. The nodal points of both glenses can be located at arbitrary positions; we call the corresponding position vectors $\mathbf{N}_1$ and $\mathbf{N}_2$. We then choose an arbitrary position $\mathbf{Q} = (x, y, z)^\top$, which gets successively imaged first by glens 1 to an intermediate position $\mathbf{Q}'$, then by glens 2 to the position $\mathbf{Q}''$. We calculate this position by applying Eq. (3) in Ref. [5] twice, once for each imaging event. If the identity-mapping condition is satisfied, then $\mathbf{Q}'' = \mathbf{Q}$, or

$$\mathbf{Q}'' - \mathbf{Q} = \mathbf{0}. \tag{5}$$

After multiplication by a common denominator, this equation takes the form of three polynomials—one for each vector component—in x, y, and z, and it must hold for all object positions $\mathbf{Q}$. Hence, all coefficients of each of these polynomials must equal zero. The set of the corresponding equations is then solved simultaneously, assuming that all focal lengths are non-zero and finite. We did this in the *Mathematica* notebook `twoGlensIntersection.nb` [17].

This procedure results in a number of conditions on the glens parameters. First the nodal points for both glenses have to coincide, i.e.,

$$\mathbf{N}_1 = \mathbf{N}_2 = \mathbf{N}, \tag{6}$$

confirming our considerations in Section 4. Second,

$$\sin\,\alpha_{12} = 0, \tag{7}$$

which means that the only possible values for α_{12} are 0 and π. The two glenses therefore lie in the same plane, either on top of each other [Fig. 4(a)] or side-by-side [Fig. 4(b)]. Third, the focal lengths must satisfy the equations

$$f_2^- = f_1^+, \tag{8}$$

in the case when $\alpha_{12} = 0$, and

$$f_2^- = -f_1^+, \tag{9}$$

in the case when $\alpha_{12} = \pi$. The other focal lengths, f_2^+ and f_1^-, can be calculated from the fact that the positive and the negative focal lengths add up to the nodal distance, n [Eq. (1)].

If both glenses are lenses, i.e., if $f_1^+ = -f_1^- = f_1$ and $f_2^+ = -f_2^- = f_2$, these equations become simply $f_1 = -f_2$ and $f_1 = f_2$. These are the cases discussed at the start of this section, in which the focal powers add up to zero ($f_1 = -f_2$), and the two lenses being equivalent to two parts of the same lens ($f_1 = f_2$). The combinations of two glenses that satisfy the identity-mapping condition can thus be said to be generalizations of these well-known lens combinations.

B. Three Glenses

It is instructive to show first that, in a combination of three glenses in given planes and with a given common nodal-point position N, only a single focal length can be arbitrarily chosen, and all other focal lengths follow. In Fig. 5, the three glenses are labelled as G_1 to G_3, and we choose f_1^+ to be the arbitrarily chosen focal length. Consider a light ray incident on G_1, from the negative side. The value that was chosen for f_1^+ then determines the direction of the ray between G_1 and G_2; this direction is constructed in Fig. 5. For the combination of the three glenses to perform the identity map, the ray needs to continue along its original straight-line trajectory after transmission through all three glenses, that is, behind G_3. But this completely determines how G_2 and G_3 must change the direction of the ray: G_2 needs to change the ray direction so that it aims for the intersection point of the initial straight-line trajectory and G_3, and G_3 needs to redirect it so that it travels in the initial direction again. This, in turn, determines f_2^+ and f_3^+. But as N is known, all nodal distances are also known, and from the nodal distances and the positive focal lengths, all negative focal lengths can be calculated. This argument can be repeated with an initial choice of one of the other focal lengths, with the same result, namely that all the other focal lengths then follow from this. Once the glens planes and the nodal-point position have been chosen, there is therefore only a single degree of freedom in a three-glens combination that performs the identity map.

To calculate the relationship between the focal lengths in a three-glens combination that performs the identity map, we consider three glenses intersecting along a line. We could try to apply this complete analogy to the case of the two-glens combination, i.e., by taking an arbitrary object position, imaging this successively through all three glenses, and then requiring the resulting image position to equal the original object position. However, we use here a different method that results in a set of simpler equations. If the identity-mapping condition is satisfied, and we choose an object position P to lie on the first glens, then this first glens images P back to itself (as glenses do not offset light rays on transmission, they image every point on the glens back to itself), and so the combination of the remaining two glenses, glenses 2 and 3, must image P back to itself. This is equivalent to saying that the image of P due to glens 2 has to equal the image of P due to glens 3. Note that no iterated imaging is required, resulting in simpler equations. Furthermore, as P lies in a plane, namely the plane of glens 1, it can be parametrized by only two coordinates, say u_1 and v_1. This yields a set of three equations, each of which can be written in the form of a polynomial in u_1 and v_1 being equal to zero. Repeating the same procedure with object positions that lie on the other two glenses, respectively parametrized by parameter pairs (u_2, v_2) and (u_3, v_3), yields another two sets of three equations each. Setting all polynomial coefficients individually to zero yields another large set of equations.

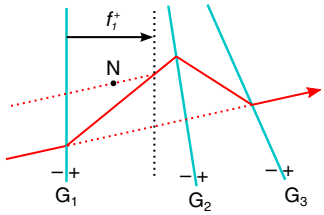

Fig. 5. Ray trajectory (red line) through three glenses, G_1 to G_3, which, in combination, perform the identity mapping. After transmission through all three glenses, the ray is restored to its original straight line. Due to the common nodal-point position N of the three glenses, the ray remains in the plane that includes the incident ray and N.

The *Mathematica* notebook `threeGlensIntersection.nb` [17] contains this calculation. The geometry of the intersection of the three glenses is as shown in Fig. 3. If the sine of one of the angles α_{ij} equals zero, then the combination of glenses i and j acts like a single glens (see Appendix B), reducing the three-glens case to the two-glens case already treated above. For the case in which the sines of all angles α_{ij} are non-zero, the results can be reduced into the following set of equations:

$$\mathbf{N}_1 = \mathbf{N}_2 = \mathbf{N}_3, \tag{10}$$

$$-f_1^- f_2^- f_3^- = f_1^+ f_2^+ f_3^+, \tag{11}$$

$$-\frac{f_1^+}{\sin\,\alpha_{12}} = \frac{f_3^-}{\sin\,\alpha_{23}}, \quad \frac{f_3^+}{\sin\,\alpha_{13}} = \frac{f_2^-}{\sin\,\alpha_{12}}, \quad \frac{f_1^-}{\sin\,\alpha_{31}} = \frac{f_2^+}{\sin\,\alpha_{32}}. \tag{12}$$

The first of these equations, Eq. (10), states that the nodal points of each of the glenses must coincide. This confirms our findings from Section 4.

Equation (11) can be interpreted by recalling that glenses are ideal thin lenses that additionally strain image space in the axial direction by a factor $\eta = -f_i/f_o$, where f_i and f_o are the image- and object-sided focal lengths [11]. Dividing both sides of Eq. (11) by the product of all positive focal lengths and replacing $-f_1^-/f_1^+$ by η_1, $-f_2^-/f_2^+$ by η_2, and $-f_3^-/f_3^+$ by η_3, the equation becomes

$$\eta_1\eta_2\eta_3 = 1, \tag{13}$$

and so the combined strains in the axial directions of all three glenses cancel out.

The equations in the set (12) share a pattern. Each equation corresponds to a preferred glens, which is glens 2 in the case of the first equation in the set. The two sides of the equation can then be constructed by picking one of the two other glenses, for example glens 1 in the case of the left-hand side, and dividing the focal length of that glens that corresponds to the side facing the preferred glens, here f_1^+, by the sine of the angle from the preferred glens to the other glens, here $\sin(-\alpha_{21}) = -\sin\alpha_{12}$. Clearly, the right-hand side of the equation corresponds to the combination of glenses 2 and 3, and the second and third equations correspond to the choice of glens 1 and glens 3 as preferred glens, respectively. It is worth noting that the third equation in the set can be shown to follow from Eq. (11) and the first two equations in the set.

Note that the resulting set of equations is a set of *necessary* conditions equivalent to the identity-mapping condition. Fortunately, this set of conditions is also *sufficient*. This can be shown as follows. We assume that the conditions derived above are satisfied, i.e., that any point on any of the glenses is imaged, by the combination of the other two glenses, to itself. From the facts that glens 1 images any point on itself back to itself and that glenses 2 and 3 image any point on glens 1 to itself, it is clear that the combination of glenses 1, 2, and 3 images any point in the plane of glens 1 to itself. Similarly, the combination of glenses 1, 2, and 3 images any point in the plane of glens 3 to itself. From the theorem derived in Appendix A, it is then clear that the combination of glenses 1, 2, and 3 images *every* point to itself. This then means that the identity-mapping condition is satisfied.

C. Four Glenses

From Section 4, we know that, in any combination of glenses that satisfies the identity-mapping condition, the nodal points of all four glenses must lie on a single straight line. We have attempted to find corresponding general conditions on the focal lengths, assuming that all four glenses intersect along a common line, but so far without success. However, we are aware of a number of solutions that apply when all four glenses are actually lenses, i.e., in the special case when each glens' negative focal length equals the negative of its positive focal length. In the following, we briefly review these solutions.

The first solution is a combination of four lenses that share an optical axis [Fig. 6(a)] and that form a paraxial cloak [18], sometimes called the *Rochester cloak*. As each lens admits a description

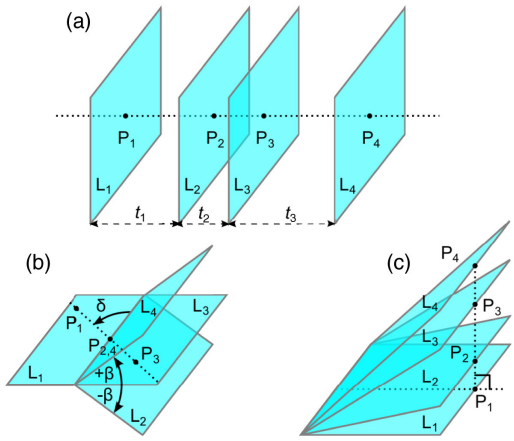

Fig. 6. Geometry of four-lens intersections for which the conditions on the focal lengths for satisfying the identity-mapping condition are known. (a) Four-lens paraxial cloak ("Rochester cloak") [18]; (b,c) different four-lens intersection lines in the ideal-thin-lens structure that forms an omnidirectional transformation-optics device [13]. The lenses are marked L_1 to L_4; P_1 to P_4 are their principal points, which are also their nodal points.

in terms of an ABCD matrix, the equations governing the system as a whole can also be written in terms of an overall ABCD matrix containing elements written as functions of the focal lengths f_i ($i = 1, \ldots, 4$) of the lenses and the distances t_j between neighboring lenses ($j = 1, 2, 3$; t_j is the distance between lenses j and $j+1$). Only symmetric combinations of lenses were studied, in which $f_1 = f_4$, $f_2 = f_3$, and $t_1 = t_3$. The overall ABCD matrix was equated to a matrix representing translation by the distance from the first to the last lens (this distance is $2t_1 + t_2$), which is equivalent to demanding that the lens combination returns every ray to its original straight-line trajectory, which in turn is equivalent to demanding that the lens combination performs the identity mapping, i.e., maps every object position to itself. This can, of course, be seen as an application of the edge-imaging condition corresponding to a loop around the common edge that starts in front of lens L_1, intersects all four lenses close to the optical axis in order of their number, and then returns, sufficiently far from the optical axis to be outside of the aperture of all lenses, to the start of the loop. The resulting relationships between the focal lengths and lens distances are

$$t_1 = f_1 + f_2, \tag{14}$$

$$t_2 = \frac{2f_2(f_1+f_2)}{f_1-f_2}, \tag{15}$$

$$2t_1 + t_2 = \frac{2f_1(f_1+f_2)}{f_1-f_2}. \tag{16}$$

Of course, the principal points of the lenses (i.e., their nodal points) all lie on a straight line, namely the optical axis.

The second special case we consider is a mirror-symmetric arrangement of lenses in which two of the lenses, L_1 and L_3, lie in the mirror plane and the other two, L_2 and L_4, lie at angles $\pm\beta$ with respect to the mirror plane [Fig. 6(b)]. The principal points

of all four lenses lie on a straight line in the mirror plane at an angle δ from the line where all four lenses intersect. Application of the identity-mapping condition yields the equations

$$\frac{f_3}{f_1} = \frac{h_3}{h_1}, \tag{17}$$

$$f_4 = \frac{f_1(2f_3\ \cos\ \beta + h_3\ \sin\ \beta \sin\ \delta)}{f_3 - f_1}, \tag{18}$$

where h_1 and h_3 are the respective distances of the principal points of lenses L_1 and L_3 from the common principal-point position of lenses L_2 and L_4.

In another special case, shown in Fig. 6(c), the lenses all intersect along a common edge, and once again the principal points all lie on a straight line, which is perpendicular to the plane of lens 1 and located a distance x_0 from the common edge. If y_i is the height of the principal point of lens i above the plane of lens 1, the conditions on the focal lengths can be written in the form [13]

$$\begin{aligned} f_4 &= f_1 \frac{s_1 \Delta y_{4,3} \Delta y_{4,2}}{s_4 \Delta y_{3,1} \Delta y_{1,2}} + \frac{x_0 \Delta y_{4,3} \Delta y_{4,1}}{s_4 \Delta y_{3,1}}, \\ f_3 &= -f_1 \frac{s_1 \Delta y_{4,3} \Delta y_{3,2}}{s_3 \Delta y_{4,1} \Delta y_{1,2}}, \\ f_2 &= f_1 \frac{s_1 \Delta y_{4,2} \Delta y_{3,2}}{s_2 \Delta y_{4,1} \Delta y_{1,3}} - \frac{x_0 \Delta y_{2,3} \Delta y_{2,1}}{s_2 \Delta y_{3,1}}, \end{aligned} \tag{19}$$

where

$$\Delta y_{i,j} = y_i - y_j \quad \text{and} \quad s_i = \sqrt{x_0^2 + y_i^2}. \tag{20}$$

D. Regular Star of Lenses

Consider n lenses with a common focal length f and a common principal point P arranged into a regular star, i.e., the lenses share a common edge through P, and all angles between neighboring lenses are the same (Fig. 7). We place a Cartesian coordinate system with its origin at P and orientated so that the z-axis coincides with the common lens edge and the x-axis points in the direction of the first lens' optical axis. The optical axis of the i-th lens then lies in the (x, y) plane, at an angle $\varphi_i = 2\pi i/n$ to the x-axis.

For simplicity, we first consider the problem in 2D, orthographically projected into the (x, y) plane. We place an Argand plane into the (x, y) plane and describe object and image positions by complex numbers $z = x + \mathrm{i}y$. Imaging by the first lens, whose optical axis coincides with the x (real)-axis, can then be described by the equation

$$z' = z \frac{f}{f - \Re(z)}, \tag{21}$$

where z and z' are the complex numbers describing the object and image positions, respectively. If the optical axis of the lens makes an angle φ with the x-axis, then it will instead hold that

$$z' = z \frac{f}{f - \Re(z\mathrm{e}^{-\mathrm{i}\varphi})}. \tag{22}$$

Now consider successive imaging of a point z_0, first by a lens with the optical-axis angle $\varphi = \varphi_0$ to a point z_1, then imaging of z_1 by a lens with the optical-axis angle $\varphi = \varphi_1$ to a point z_2, etc., up to the lens with angle $\varphi = \varphi_{n-1}$ to a point z_n. What can we say about the position of the point z_n with respect to z_0? To see it, we make a substitution

$$z_i = w_i \frac{z_0}{|z_0|}. \tag{23}$$

Clearly, $w_0 \in \mathbb{R}$. For the sequence of w_i we then get

$$w_{i+1} = w_i \frac{f}{f - \Re(w_i \mathrm{e}^{-\mathrm{i}\varphi_i} z_0/|z_0|)}, \tag{24}$$

from which it follows that also all $w_i \in \mathbb{R}$. We can now rewrite the last equation into the form

$$\frac{f}{w_i} - \frac{f}{w_{i+1}} = \frac{\Re(w_i \mathrm{e}^{-\mathrm{i}\varphi_i} z_0/|z_0|)}{w_i}. \tag{25}$$

Now, since w_i is real, we can remove it from the numerator and denominator, getting

$$\frac{f}{w_i} - \frac{f}{w_{i+1}} = \Re[\mathrm{e}^{\mathrm{i}(\psi - \varphi_i)}] = \cos(\varphi_i - \psi), \tag{26}$$

where we have denoted $\psi = \arg(z_0/|z_0|)$. This equation holds for $i = 0, 1, \ldots, n-1$. Summing all these equations, we get

$$\frac{f}{w_0} - \frac{f}{w_n} = \sum_{i=0}^{n-1} \cos(\varphi_i - \psi) = 0, \tag{27}$$

where the last equality holds due to the uniform angular distribution of the angles φ_i. This proves that $w_n = w_0$ and hence also $z_n = z_0$, which we wanted to prove—every point is imaged back to itself by this lens combination.

To go now to the 3D case, we note that everything we wrote about the 2D case holds for the projection of the 3D case along the edge where all the lenses meet to the plane perpendicular to that edge and that also all the image points from the sequence lie on a straight line through the common nodal point. Then it follows immediately that also the "vertical position" of the last image point will be the same as that of the object point.

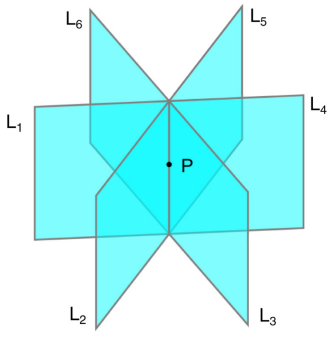

Fig. 7. Regular star of lenses. Any number of lenses can form a regular star; the figure is drawn for six lenses. All lenses have the same focal length, f, and principal point, P, and intersect along a common edge through P. All angles between neighboring lenses are equal; in a star of n lenses, neighboring lenses are at an angle $2\pi/n$.

For the case of an even number of lenses, the result that the lens star satisfies the identity-mapping condition can be derived very easily from the fact that a combination of two lenses that share a common nodal point performs the same mapping, irrespective of the order of the two lenses, derived in Appendix C, as follows. By definition, all lenses share a nodal point, which means that the order in which light passes through two neighboring lenses is irrelevant. By repeatedly swapping of the order of pairs of neighboring lenses means that any lens can be brought next to any other lens. Specifically, in a regular lens star with an even number of lenses, any lens at an angle α can be brought next to the lens $\alpha + \pi$ it is diametrically opposite to, which can be seen as the other half of that lens. But we know that two lenses that are actually two halves of the same lens satisfy the identity-mapping condition, and so the effects of these two lenses cancel each other. Thus, we have effectively reduced the number of lenses in the lens star by 2. But as every lens in the regular star of an even number of lenses has an opposite number, the effect of *all* lenses can be cancelled in this way until we are left with the identity mapping. Note that this means that a regular lens star with an even number of lenses in which opposite pairs of lenses are missing also satisfies the identity-mapping condition.

6. APPLICATION

The results from this paper enabled our previous work on glens-based [9] and ideal-lens-based [13,14] TO devices. Here we briefly outline the process by which we designed the ideal-lens structure that is the basis of both the omnidirectional lens [13] and ideal-lens cloaks [14], highlighting the use of this paper's results.

We decided to design first a 2D ideal-lens TO structure, as follows. We started by considering a simple ideal-lens structure, such as the one shown in Fig. 8(a). We applied the nodal-point conditions, derived in Section 4, to place the principal points (which, in the case of ideal lenses, coincide with the nodal points) of all lenses, and we found that the conditions could not be satisfied. In the case of the structure shown in Fig. 8(a), this is because each lens ends in two three-lens intersections,

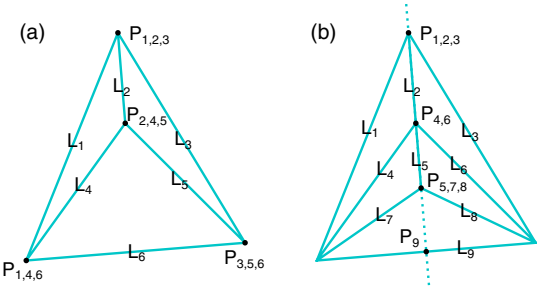

Fig. 8. Placement of the principal points (which, in ideal lenses, coincide with the nodal points) according to the nodal-point conditions (Section 4) in structures of ideal lenses (cyan lines). $P_{i,j,\ldots}$ is the principal point (and therefore the nodal point) of lenses L_i, L_j, …, placed so that the nodal-point conditions are satisfied for the intersections involving any of those lenses. (a) Example of a structure in which the conditions require one or more principal points, i.e., that of lens L_1, to lie in two positions at the same time. In such structures, the nodal-point conditions cannot be satisfied. (b) Structure in which the nodal-point conditions can be satisfied.

which means that each lens's principal point must lie on both three-lens intersections in which that lens participates, which is clearly impossible. By repeating this process of elimination with different structures, we arrived at the structure shown in Fig. 8(b), in which the nodal-point conditions could be satisfied. This structure is the 2D version of the omnidirectional lens [13] and the ideal-lens cloak [14].

The next steps were to generalize the 2D ideal-lens structure to 3D; to collect the relevant equations, derived in Section 5, for the focal lengths of the lenses involved in the various types of lens intersections in the 3D structure into a set of equations; and to solve this set of equations. We obtained infinitely many different solutions, which we discuss in Refs. [13,14].

7. CONCLUSIONS

The results presented in this paper already proved invaluable in our own work on constructing TO devices from glenses and lenses. We used these results at two stages of the design process: at the start, where they allow quick and easy placement of the nodal points, and rejection of unsuitable designs; and at the end, where they enable calculation of the full set of glens parameters.

In future, we intend to study combinations of four glenses or more that satisfy the edge-imaging condition and use such results to construct new (g)lens-based TO devices that perform specific functions.

APPENDIX A: A COLLINEATION THAT MAPS ANY POINT ON TWO PLANES TO ITSELF MAPS EVERY POINT TO ITSELF

Consider a collineation that maps any point on the two planes I_1 and I_2 to itself (Fig. 9). We want to construct the image P′ of an arbitrary position P.

First, because a collineation has the property that *every* point is mapped to a corresponding image position, there exists an image position P′. Next, we place a straight line A through P and construct the points A_1 and A_2 where it intersects I_1 and I_2, respectively. As A_1 and A_2 lie on I_1 and I_2, they are mapped to themselves, and as a collineation maps any point on straight lines onto straight lines, the straight line A, which passes through A_1 and A_2, is mapped to a straight line again, and this straight line passes through the images of A_1 and A_2, i.e., A_1 and A_2. In other words, the straight line A is mapped to itself, and as P lies on A, the image P′ of P lies on A. Repeating this argument with another straight line, B, through P immediately reveals that P′

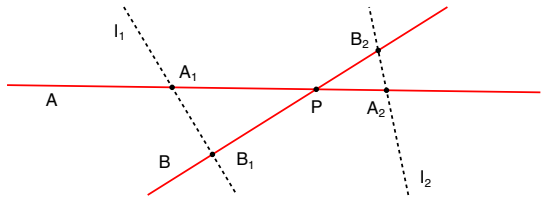

Fig. 9. Mapping of an arbitrary position P in the presence of two planes, I_1 and I_2 (dashed black lines), that have the property that any point that lies on I_1 or I_2 is mapped to itself. Two light rays (solid red lines) are placed through P; A_1 and B_1 are the intersections of these rays with I_1, and A_2 and B_2 are the intersections of these rays with I_2.

lies on the intersection point of A and B, which is the point P. We have therefore shown that *any* position P is mapped to itself.

APPENDIX B: COMBINATIONS OF TWO CO-PLANAR GLENSES AND LENSES

Consider two glenses in the same plane. The optical axes of the two glenses can be offset relative to each other, but they are parallel or antiparallel. We assume here that the optical-axis directions are parallel.

We can see immediately two properties of this glens combination:

1. Any object position is imaged by the first glens to an intermediate position, which is then imaged by the second glens to an image position. The combination therefore images every position to a corresponding position.
2. Each glens changes the direction of transmitted rays without offsetting them. The combination of two glenses in the same plane therefore does this also.

In Ref. [11], it was shown that the most general optical element that satisfies these conditions is, in fact, a glens (a term that was not defined until later [5]).

To construct the optical axis and cardinal points of this equivalent glens, we consider Fig. 10(a), which shows two co-planar glenses, G_1 and G_2, along with their focal points and a number of principal rays passing through the combination from the side of G_1. We now consider these light rays in turn.

Light ray 1 is chosen so that, between the glenses, it travels along the straight line between F_1^+, the image-sided focal point of G_1, and F_2^-, the object-sided focal point of G_2. After passage through G_1, it is headed for F_1^+, which means that before passage through G_1, it must have travelled parallel to G_1's optical axis. It approaches G_2 from the direction of F_2^-, which means that G_2 redirects it in a direction parallel to its optical axis. As the glenses are co-planar, their optical-axis directions are, of course, the same, and this optical-axis direction is also that of the equivalent glens. Light ray 1 therefore travels in the optical-axis direction before and after the combination, so it must travel along the optical axis of the equivalent glens. We can therefore place the principal point P of the equivalent glens at the intersection between the plane of the glenses and the line through F_1^+ and F_2^-.

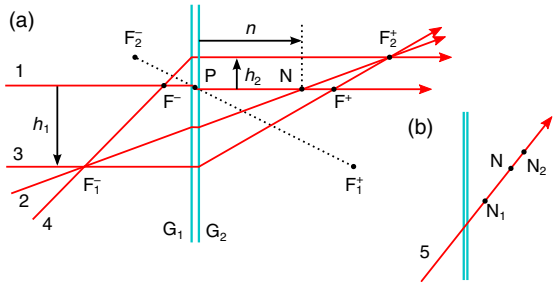

Fig. 10. Diagrams relating to properties of co-planar glenses (cyan lines). The trajectories of a few principal rays are shown (red arrows). (a) Diagram used in the construction of the cardinal points of co-planar glenses, G_1 and G_2. F_1^- and F_1^+, F_2^- and F_2^+, and F^- and F^+ are the object- and image-sided focal points of glenses G_1, G_2, and of the glens equivalent to the combination, respectively. N is the nodal point of the equivalent glens. For clarity, the glenses are drawn slightly apart. (b) The principal ray through the nodal points N_1 and N_2 of the individual glenses.

Light ray 2 travels along the straight line between F_1^- and F_2^+. As it approaches G_1 from F_1^-, G_1 redirects it in a direction parallel to the optical axis, so G_2 redirects it toward F_2^+. But as it already travelled toward F_2^+ when it approached the glens combination, it passes through the combination undeviated. This implies that the nodal point N of the combined glens must lie on this ray. N also lies on the optical axis, so it must lie at the intersection point of light rays 1 and 2.

Ray 3 is chosen so that it approaches G_1 along its optical axis. It therefore passes straight through G_1, approaches G_2 parallel to its optical axis, and therefore passes through F_2^+. As it approached the combination parallel to its optical axis, it passes through its image-sided focal point, F^+, which therefore lies at the intersection of light rays 1 and 3. Similarly, the object-sided focal point F^- of the equivalent glens lies at the intersection of rays 1 and 4, the latter chosen so that, after passage through both glenses, it travels along the optical axis of G_2.

We can now calculate the nodal distance, n, of the equivalent glens. The glens combination is equivalent to an ideal lens when $n = 0$. We define h_1 to be the distance of the optical axis G_1 *above* that of the equivalent glens [note that Fig. 10(a) is drawn for the case $h_1 < 0$]; similarly, h_2 is the distance of G_2's optical axis above that of the equivalent glens.

To calculate the nodal distance n of the equivalent glens, we consider the similar right triangles with their base coinciding with the optical axis of G_1 and hypotenuse F_1^-N and $F_1^-F_2^+$, respectively. We can solve the equation

$$\frac{h_2 - h_1}{f_2^+ - f_1^-} = \frac{-h_1}{n - f_1^-} \tag{B1}$$

for n, obtaining

$$n = \frac{f_1^-(h_2/h_1) - f_2^+}{h_2/h_1 - 1}. \tag{B2}$$

From the similar right triangles with their base coinciding with the optical axis of the equivalent glens and hypotenuse F_2^-P and F_1^+P, respectively, we see that

$$\frac{h_2}{h_1} = \frac{f_2^-}{f_1^+}. \tag{B3}$$

Substitution into Eq. (B2) reveals

$$n = \frac{f_1^- f_2^+ - f_1^+ f_2^-}{f_1^+ - f_2^-}. \tag{B4}$$

If the two glenses are actually lenses, $f_1^+ = -f_1^- = f_1$ and $f_2^+ = -f_2^- = f_2$, and so

$$n = \frac{-f_1 f_2 + f_1 f_2}{f_1 + f_2} = 0. \tag{B5}$$

This means that any combination of co-planar lenses can be described by an effective lens.

It can easily be shown that the two focal lengths f^- and f^+ of the combination are then given by the equations

$$\frac{1}{f^-}=\frac{1}{f_1^-}+\frac{1}{f_2^-},\qquad \frac{1}{f^+}=\frac{1}{f_1^+}+\frac{1}{f_2^+}. \tag{B6}$$

This is, of course, in complete analogy to the standard formula for the focal powers of two lenses adding up.

It is now easy to show that N glenses in the same plane also act like a single glens and that the negative and positive focal powers of this combination are

$$\frac{1}{f^-}=\sum_{i=1}^{N}\frac{1}{f_i^-},\qquad \frac{1}{f^+}=\sum_{i=1}^{N}\frac{1}{f_i^+}. \tag{B7}$$

Finally, we consider light ray 5 (Fig. 10), chosen to pass through the nodal points N_1 and N_2 of both individual glenses. As the ray passes through the nodal points of both glenses, it passes through the combination undeviated. This, in turn, implies that this ray also passes through the nodal point N of the equivalent glens. We have thus shown that the nodal points N_1, N_2, and N lie on a straight line.

APPENDIX C: A COMBINATION OF TWO LENSES THAT SHARE A COMMON NODAL POINT PERFORM THE SAME MAPPING, IRRESPECTIVE OF ORDER

We start with the equation, derived in Ref. [5], for the position $\mathbf{Q}'$ of the image of a point $\mathbf{Q}$ by a lens with optical-axis direction $\hat{\mathbf{a}}$, nodal point $\mathbf{N}$, and focal length (more specifically a coordinate of the image-sided focal point) f:

$$\mathbf{Q}'=\mathbf{Q}+\frac{(\mathbf{Q}-\mathbf{N})\cdot\hat{\mathbf{a}}}{f-(\mathbf{Q}-\mathbf{N})\cdot\hat{\mathbf{a}}}(\mathbf{Q}-\mathbf{N}). \tag{C1}$$

Without loss of generality, we choose our coordinate system so that the origin coincides with the nodal point, $\mathbf{N}$; that the two lenses intersect along the y-axis; and that the normalized normal to the first lens is simply

$$\hat{\mathbf{a}}_1=\hat{\mathbf{z}}. \tag{C2}$$

The normalized normal to the second lens is

$$\hat{\mathbf{a}}_2=\begin{pmatrix}-\sin\alpha\\0\\\cos\alpha\end{pmatrix}. \tag{C3}$$

It can be shown (we used *Mathematica* [19]) that successive imaging of a general point

$$\mathbf{Q}=\begin{pmatrix}x\\y\\z\end{pmatrix}, \tag{C4}$$

first by lens 1 (focal length f_1), then by lens 2 (focal length f_2), gives the image position

$$\mathbf{Q}'=\frac{f_1 f_2}{f_2(f_1-z)-f_1 z\cos\alpha+f_1 x\sin\alpha}\mathbf{Q}. \tag{C5}$$

Successive imaging of $\mathbf{Q}$ first by lens 2, then by lens 1, gives the same image position.

Funding. Engineering and Physical Sciences Research Council (EP/K503058/1, EP/M010724/1, EP/N/509668/1).

Disclosures. The authors declare no conflicts of interest.

REFERENCES

1. U. Leonhardt, "Optical conformal mapping," Science **312**, 1777–1780 (2006).
2. J. B. Pendry, D. Schurig, and D. R. Smith, "Controlling electromagnetic fields," Science **312**, 1780–1782 (2006).
3. R. F. Stevens and T. G. Harvey, "Lens arrays for a three-dimensional imaging system," J. Opt. A **4**, S17–S21 (2002).
4. A. C. Hamilton and J. Courtial, "Metamaterials for light rays: ray optics without wave-optical analog in the ray-optics limit," New J. Phys. **11**, 013042 (2009).
5. G. J. Chaplain, G. Macauley, J. Bělín, T. Tyc, E. N. Cowie, and J. Courtial, "Ray optics of generalized lenses," J. Opt. Soc. Am. A **33**, 962–969 (2016).
6. J. Courtial, S. Oxburgh, and T. Tyc, "Direct, stigmatic, imaging with curved surfaces," J. Opt. Soc. Am. A **32**, 478–481 (2015).
7. S. Oxburgh, C. D. White, G. Antoniou, E. Orife, and J. Courtial, "Transformation optics with windows," Proc. SPIE **9193**, 91931E (2014).
8. S. Oxburgh, C. D. White, G. Antoniou, E. Orife, T. Sharpe, and J. Courtial, "Large-scale, white-light, transformation optics using integral imaging," J. Opt. **18**, 044009 (2016).
9. T. Tyc, S. Oxburgh, E. N. Cowie, G. J. Chaplain, G. Macauley, C. D. White, and J. Courtial, "Omni-directional transformation-optics cloak made from lenses and glenses," J. Opt. Soc. Am. A **33**, 1032–1040 (2016).
10. A. C. Hamilton and J. Courtial, "Generalized refraction using lenslet arrays," J. Opt. A **11**, 065502 (2009).
11. J. Courtial, "Geometric limits to geometric optical imaging with infinite, planar, non-absorbing sheets," Opt. Commun. **282**, 2480–2483 (2009).
12. T. Maceina, G. Juzeliūnas, and J. Courtial, "Quantifying metarefraction with confocal lenslet arrays," Opt. Commun. **284**, 5008–5019 (2011).
13. J. Courtial, T. Tyc, J. Bělín, S. Oxburgh, G. Ferenczi, E. N. Cowie, and C. D. White, "Ray-optical transformation optics with ideal thin lenses makes omnidirectional lenses," Opt. Express **26**, 17872–17888 (2018).
14. J. Bělín, T. Tyc, M. Grunwald, S. Oxburgh, E. N. Cowie, C. D. White, and J. Courtial, "Ideal-lens cloaks and new cloaking strategies," Opt. Express (to be published).
15. J. C. Miñano, "Perfect imaging in a homogeneous three-dimensional region," Opt. Express **14**, 9627–9635 (2006).
16. A. Hendi, J. Henn, and U. Leonhardt, "Ambiguities in the scattering tomography for central potentials," Phys. Rev. Lett. **97**, 073902 (2006).
17. J. Courtial, T. Tyc, S. Oxburgh, J. Bělín, E. N. Cowie, and C. D. White, "Mathematica notebooks with detailed loop-imaging-theorem calculations," figshare, 2016, https://dx.doi.org/10.6084/m9.figshare.4269701.v1.
18. J. S. Choi and J. C. Howell, "Paraxial ray optics cloaking," Opt. Express **22**, 29465–29478 (2014).
19. J. Courtial, "Calculations about interchangeability of the order of lenses and glenses with a common nodal point," figshare, 2019, https://doi.org/10.6084/m9.figshare.10299299.v1.